Hindawi
International Journal of Rotating Machinery
Volume 2019, Article ID 4359524, 17 pages
https://doi.org/10.1155/2019/4359524

Research Article

An Investigation on Speed Control of a Spindle Cluster Driven by Hydraulic Motor: Application to Metal Cutting Machines

Ngoc Hai Tran,[1] Cung Le ,[1] and Anh Dung Ngo[2]

[1] *University of Science and Technology, University of Danang, Vietnam*
[2] *École de Technologie Supérieure (ÉTS), Canada*

Correspondence should be addressed to Cung Le; lcung@dut.udn.vn

Received 27 August 2018; Revised 21 December 2018; Accepted 31 January 2019; Published 19 February 2019

Academic Editor: Ryoichi Samuel Amano

In this article, we present an experimental study on the speed stability of a spindle driven by a hydraulic motor, which is controlled by a proportional valve, through a V-belt transmission. The research includes the dynamic modeling of the transmission cluster and the transmission from the hydraulic motor to the working shaft via V-belt mechanism, together with the establishment of a mathematical model and fuzzy self-tuning PID controller model. In the model, the V-belt is assumed as an elastic module, and the friction coefficient and mass inertia moment of the hydraulic motor are considered as constant. The Matlab software is used to simulate the speed response of the hydraulic motor to the working shaft. Based on theoretical study, we resemble the experimental system and determine the parameters for the fuzzy self-tuning PID controller. We conduct experiment and investigate the speed stability of the working shaft from 300 to 1100 (rpm) based on transient response parameters such as the time delay, the setting time, the overshoot, and the rotation error at steady state. Thereby, in this study, the simulation and the experiment results are compared and evaluated regarding the speed stability of the working shaft driven by hydraulic motor transmitted through V-belt mechanism. The findings show the speed controllability by using proportional valve to manipulate the oil flow and applying a self-tuning PID controller to achieve very good results such as the error difference of 0.001 to 0.036%, the delay of 0.01 to 0.02 seconds, no overshoot, and the settling error less than 5% compared to the set values. On the other hand, we include the effect of the oil temperature of 40 to 80°C on the working shaft speed (500, 900 rpm) in this study and derive that the system works well at temperature range of 40 to 70°C. On these findings, we propose the applicability of this system on the current machinery cutters. In addition, we verify the effects of the hydraulic drive for main shaft, controlled by fuzzy PID, by comparison of the roughness of the machining work piece with respect to the one using the 3-phase motor drive.

1. Introduction

Automatic transmission and control of hydraulic systems (ATACOHS) is one among the high technology development directions in machining and equipment industry. Due to its outstanding features such as compact structure, great torque transmission, fast response speed, self-lubricating, and heat transfer properties of liquid and good system life, the research on ATACOHS has got very high attention recently [1]. Indeed, in industrial applications, ATACOHS has been applied to cutting tools movement system by several cutting machines manufacturers [2–6]. Currently, there are two main approaches in the stepless speed control of a hydraulic motor. The first approach is to change the working mode of the pump and the hydraulic motor which can vary the volume of the pump and the motor [7] or change the speed of the pump through changing the speed of the three-phase electric motor using an inverter [8]. The other one is to change the resistance on the oil path by a proportional valve or a servo valve. This method is more commonly used because the closed loop control system has a strong relationship between the input/output response signals and the feedback signal to the controller for minimize the system errors [1, 8–13].

However, there is almost no application to the spindle cluster driven by hydraulic motors because there are many design challenges for ATACOHS: the dynamic process is a nonlinear relationship due to many factors such as the elasticity of the fluid, the relationship between the flow and

the pressure, the change in viscosity due to oil temperature [1, 14–17], the pressure loss in the pipeline, the oil leakage inside the hydraulic elements, and the influence of other nonlinear parameters during operation. Therefore, for simplicity, they usually linearized such nonlinear systems in the controller design process for an ATACOHS [9, 18].

With the rapid development of control technology and the application of that technique to ATACOHS control [19], it is possible to mention some of the applicable control methods which are feedback control, adaptive control, fuzzy logic control, neural network control, and genetic algorithm control. Thus, the problems encountered in the precise control of the ATACOHS system are no longer a concern for designers. Each controller has different characteristics, and depending on the actual requirements of the system, the designer selects a suitable control method. However, through the literature study, there are two controllers commonly used today: classic PID controllers and fuzzy PID controllers.

Classic PID controllers [1, 10, 16, 20, 21] are the most common control tools in many industrial applications, because they can improve response times and steady state errors. On the other hand, the structure of the PID sets is simple and intuitive with the K_P, K_I, K_D parameter sets. However, the K_P, K_I, K_D parameter sets are usually fixed during the operation of the system, so it is usually applied to control the hydraulic actuator operating at a fixed output value. Ming Xu et al. [10] introduced an experimental model for controlling the velocity of a hydraulic cylinder by using proportional valve in combination with a method of controlling the input speed of the pump via controlling the speed of three-phase electric motor using converter (energy saving solution). The classic PID controller was used for processing and speed controlling. The results of this study indicated accuracy in high-speed control, fast feedback, and good energy efficiency of the designed controller (at the same condition of 0.2m/s). This approach derived a very good result and can be applied in practice, but its drawback is the high cost. Furthermore, a speed control model for a conveyor belt driven by hydraulic motor through rack and pinion mechanism was introduced by Rong Li and his colleges [20]. Through the static and dynamic properties of simulation and initial system analysis, they found that the system was difficult to achieve the required control accuracy. From there, they designed the PID controller. The results show that the system response has been improved, the overshoot from over 31.2% decreased to 18.4%, the response time from 1.146s decreased to 0.0143s, the oscillation frequency from 7.4Hz decreased to 7 Hz, the error amplitude is less than 0.05%, and the phase error is less than 0.2%. K. Dasgupta et al. reported the reasonable simulation results of a hydraulic motor at a value of 50 rad/s with the PI parameter set ($K_I = 100$, $K_P = 10$).

With the consideration of the effect of oil temperature on the dynamic properties of servo valves and hydraulic motors [1, 17], A.A.M.H. AL-Assady et al. designed and analyzed the speed controller for hydraulic motors using proportional valves and a PID controller with various parameter sets of K_P, K_I, K_D which was established by using the Trial and error method, Ziegler and Nichols method, and Self-turn parameters by Matlab package. Experimental results showed that when using a classical PID controller, the desired dynamic quality is achieved when the temperature range of 60°C to 70°C at a rotational speed of 700 hydraulic rpm and the load varies on the output shaft of the hydraulic motor. Fouly A. et al. reported the effects of oil temperature on the servo motor's dynamic properties. The experiments were carried out in the case of no load and load of 5560N. The effect of hydraulic oil temperature changes on system performance was investigated starting from 28 to 500°C. The result at load (5560N) and pressure (50bar), the higher the temperatures, the faster the flow of oil through the valve (at 280°C, the flow through the valve is 48.55ml/s; at 400°C, the flow through the valve is 56,69ml/s, and at 500°C, the flow through the valve is 66,34ml/s). On the other hand, when the temperature rises, the pressure across the valve decreases. The above statements show that the PID controllers is only suitable for fixed output systems, and for systems with variable output, PID control is no longer suitable.

Applying fuzzy PID controllers [9, 12, 13, 22] significantly improves the disadvantages of classical PID controllers; it gave faster response time, no overshoot, and less steady state error. The highlight is K_P, K_I, K_D automatically adjusted in the process of operation. In particular, Kwanchai Sinthipsomboon et al. control servohydraulic valve assemblies by applying a self-adjusting fuzzy PID controller; i.e., the parameters and PID controller were adjusted using the fuzzy rule set (Zhang et al., 2004; Song and Liu, 2010; Zulfatman and Rahmat, 2006; Feng et al., 2009), the results of motor speed control of 100 rpm which was much better than that when using PID control.

Through the analysis of the above studies, we choose the self-adjusting fuzzy PID controller on the proposed model. Previous publications have studied only one spin volume and one elastic segment, which are not unique, but in real situations, there are structures with multiple spin volumes and multiple elastic properties in many practical applications.

Our difference is that we have two rotational masses and two elastic stages in the proposed model of the speed control of the hydraulic transmission work shaft. The fuzzy PID controller is design to control at various setting speeds and takes into account the oil temperature change. The results of the study are verified on the speed response of lathe axis.

The main shaft of metal cutting machine plays an important role in the machining process as it provides cutting speeds for the cutting tools and is a part of the transmission mechanism between the machine and the cutting tools or the parts. When manufacturing on metal cutting machine, manufacturers have studied this problem. However, each designed model of spindle has different characteristics. The spindle drive is the transmission mechanism of the spindle, including the drive motor. Typically, there are two main types of spindle depending on the type of drive mechanism: direct drive and indirect drive (via a belt mechanism or gear drive). In this study, we chose the belt mechanism for transmitting the motion from the hydraulic motor to the main shaft.

Based on the analysis of these studies, different research hypothesis will result in different mathematical models, and different control applications lead to variation in quality of the system dynamics. Also, as the authors aware, there is

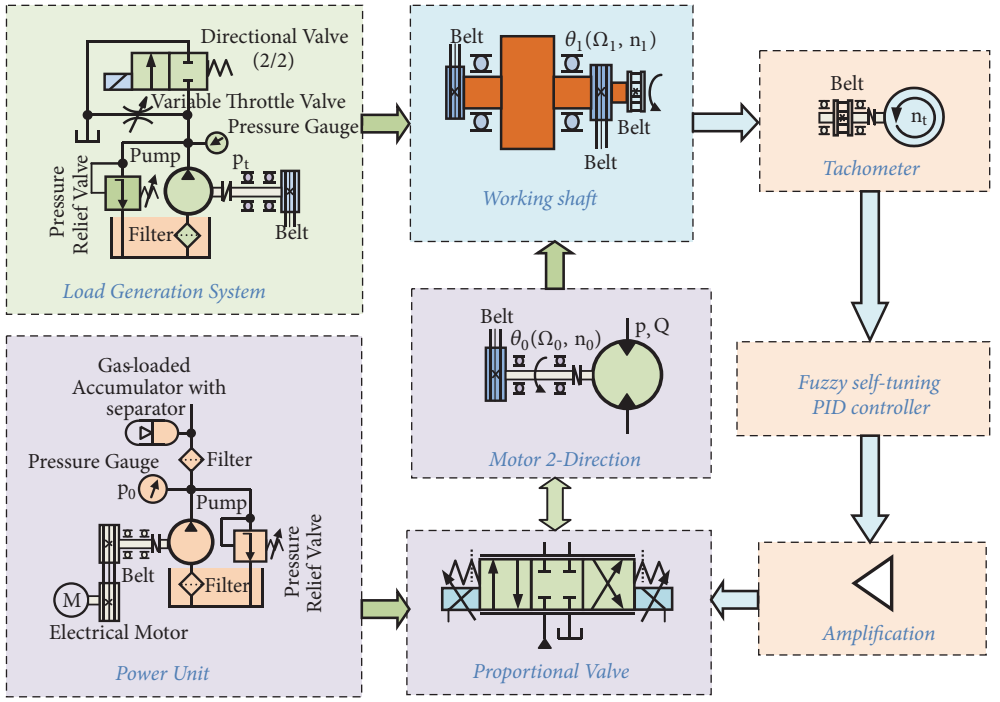

Figure 1: System configuration.

currently no publication on the application of ATACOHS drive for machinery cutters. Thus, in this study, we propose a model of spindle speed control that simulates the lathe spindle assembly. In our proposed model, we also take into account the elastic deformation of the transmission belt from hydraulic motors to working shaft, the friction, and the value of momentum inertia on the working shaft and also on the rotary axis of the hydraulic motors. The procedure is as follows: Firstly, we develop a theoretical model of spindle control, set up a dynamic computational model with assumptions, mathematical description of the system, and define the structural parameters of the system. Secondly, we fabricate and resemble the working shaft and the hydraulic transmission. Then, we develop a self-tuning PID control model, define the experimental range of the PID control parameter set, and program the system control program on the IDE software [23] and build the interface on Matlab/Guide [24, 25]. The results of the transient response of the speed stability of the work axes of the theoretical and experimental are shown graphically. The results are verified by an application in a machining equipment test.

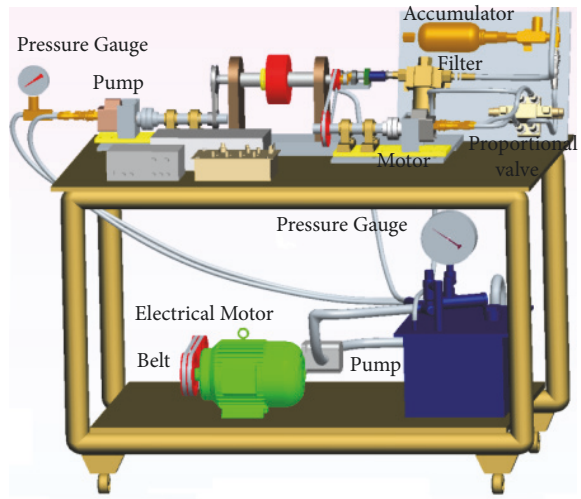

Figure 2: Experimental model.

2. Method

2.1. Research Model. The research model of the speed control of transmission cluster includes the hydraulic motor and V-belt mechanism. Figures 1 and 2 show the system configuration and experimental model of our study, respectively. In the model, three-phase electric motor drives the gear of the oil pump through a V-belt; the working pressure as well as the overflow prevention is controlled by an overflow valve and a safety valve. The speed of a hydraulic motor is regulated by the oil flow which is controlled by proportional valve [1, 10, 26]. On the oil line from the pump to the proportional valve, there are a high-pressure filter and the battery to accumulate and compensate for the oil potential energy [10, 27, 28].

In addition, a hydraulic motor transmits rotation to the working shaft through a V-belt; the speedometer of the working shaft is used as a speed sensor to measure the speed. The speedometer receives the speed signal of the working shaft through the transmission belt. We use the oil pump as the load equipment. The load can be changed by changing the pressure (p_t) by using overflow valve and safety valve.

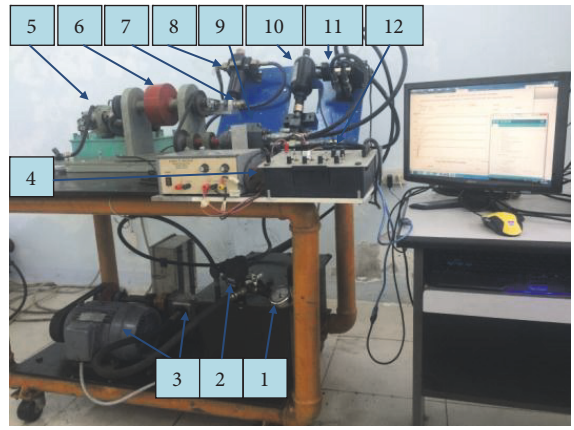

Figure 3: Picture of experimental system (1: pressure gauge; 2: overflow valve and safety valve (maximum pressure $31.10^6 N/m^2$, maxiumum flow rate 56.7l/min, Taiwan); 3: hydraulic power with three-phase motor (2.2 kW, 1420 rpm) operating with the V-belt (transmission ratio is 1:1) to supply oil for gears (volume is $12*10^{-6} m^3/rev$; maximum pressure is $20*10^6 N/m^2$); flow rate supplying for the system is 17.04l/min; 4: amplification (Festo Didactic); 5: load generation system; 6: working shaft; 7: tachometer (Pittman USA, no F8412G591, 2V/Krpm); 8: high-pressure filter. Using to filter debris of oil (Parker, USA); 9: Hydraulic motor ($12*10^{-6} m^3/rad$, Rockford illinois, Model 16-Z-3); 10: hydraulic accumulator ($34*10^6 N/m^2$, volume 0.95l); 11: proportional valve ($Q = 0 \div 2.33*10^{-4} m^3/s$, $p_{max} = 15.98*10^6 N/m^2$, $I_{max} = 100$ mA, input voltage 0÷24 VDC, linear error < 4%, Festo Didactic Proportional valve 4/3); 12: Arduino (MEGA 2560); digital-to-analog converter (DAC 4921)).

Based on the theory mentioned before, the test-rig for the experimental tests is built and shown in Figure 3.

2.2. Mathematical Model. The mathematical model of ATACOHS system is established based on linear system assumption [9, 18]. Both the elastic deformation of the transmission belt from the rotary shaft of the hydraulic motor to the working axis and the friction and the moment of inertia on the rotor of the hydraulic motor are included (the values in the hypothesis are chosen from the manufacturer catalog or by measurements). Due to a very small load and nonelastic of belt, the transmission of the belt conveyor from working shaft to speed sensor is considered as a proportional module. The analysis model of ATACOHS is shown in Figure 4, and the system parameters are shown in Table 1.

With the established mathematical model and the hypotheses of the system dynamics, we describe the mathematical formulation of the system as follows:

On the working shaft:

(i) The moment on the working shaft [29]:

$$\left(T_1 - T_2\right).r_1 = J_1.\frac{d^2\theta_1}{dt^2} + f_1.\frac{d\theta_1}{dt} + M_L; \quad \left(M_L = p_t D_b^t\right) \tag{1}$$

(ii) Belt horsepower [29]:

$$T_1 = k.\left(r_0.\theta_0 - r_1.\theta_1\right); \quad T_2 = k.\left(r_1.\theta_1 - r_0.\theta_0\right) \tag{2}$$

(iii) Feedback:

$$F = K_n.n_t = K_n.n_1; \quad n_t = n_1; \left(\frac{n_t}{n_1} = 1\right) \tag{3}$$

On the hydraulic motor [1, 8, 9, 18]:

(i) The moment of rotor of the hydraulic motor:

$$D_m^0.p = J_0.\frac{d^2\theta_0}{dt^2} + f_0.\frac{d\theta_0}{dt} + \left(T_1 - T_2\right).r_0 \tag{4}$$

(ii) Flow:

Hydraulic motor:

$$Q = D_m.\frac{d\theta_0}{dt} + c.\frac{dp}{dt} + \lambda.p \quad \left(c = \frac{V_1 + V_2}{2B},\ D_m = \frac{D_m^0}{2\pi}\right) \tag{5}$$

Proportional valve:

$$Q = K_V.I \quad \text{(neglecting the flow loss of the valve)} \tag{6}$$

From (1) to (6), we can obtain

$$2k.r_1.\left(r_0.\theta_0 - r_1.\theta_1\right) = J_1.\frac{d^2\theta_1}{dt^2} + f_1.\frac{d\theta_1}{dt} + M_L$$

$$D_m^0.p = J_0.\frac{d^2\theta_0}{dt^2} + f_0.\frac{d\theta_0}{dt} + 2k.r_0.\left(r_0.\theta_0 - r_1.\theta_1\right)$$

$$Q = D_m.\frac{d\theta_0}{dt} + c.\frac{dp}{dt} + \lambda.p$$

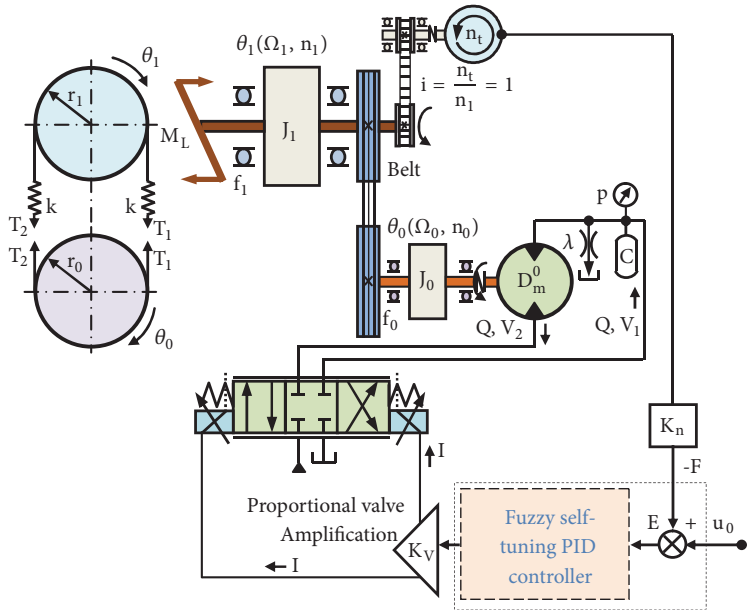

Figure 4: Mathematical model.

Table 1: System parameters.

Symbol	Specifications of the (ATACOHS)			
	Description	*Source of Information*	*Unit*	*Value*
D_m	Motor displacement	Manufacturer data	m^3/rad	$12*10^{-6}$
$V_1 + V_2$	Total fluid volume in pipes	Calculated	m^3	$20.5*10^{-5}$
B	Hydraulic bulk modulus	Manufacturer data	N/m^2	$14*10^8$
λ	Leakage coefficient of motor	Calculated experimentally	m^5/Ns	$2.5*10^{-11}$
k	Stiffness of the V-belt	Calculated experimentally	N/m	20
r_1	Radius of driven pulley	Manufacturer data	m	0.09
r_0	Radius of drive pulley	Manufacturer data	m	0.09
J_1	Inertia of load	Calculated	Nms^2/rad	$45*10^{-3}$
J_0	Inertia of motor	Calculated	Nms^2/rad	$3.5*10^{-3}$
T_1, T_2	Tension on the belt	Calculated	N	-
Q	Input and output flow rate of the hydraulic motor	From experimental	m^3/s	-
p	Supply pressure	From experimental	N/m^2	$49*10^5$
I	Current of proportional vales (maximum)	Manufacturer data	mA	100
n_0	Rotor speed	experimentally	rpm	-
n_1	Working shaft speed	experimentally	rpm	-
K_V	Valve flow gain	Manufacturer data	$(m^3/s)/mA$	$11.5*10^{-3}$
θ_0	Rotation angle of rotor	Manufacturer data	rad	-
θ_1	Rotation angle of working shaft	Manufacturer data	rad	-
K_n	Tachogenerat or gain	Calculated experimentally	V/rpm	0.0167
u_0	Control voltage	Manufacturer data	vDC	$0\div\pm10$
u_1	Valve control voltage	Manufacturer data	vDC	$0\div\pm24$
f_0	equivalent viscous coefficient of motor	Calculated experimentally	Nms/rad	$29.5*10^{-4}$
f_1	Friction coefficient of working shaft	Calculated experimentally	Nms/rad	0.118
M_L	Load on working shaft	Calculated experimentally	Nm	-

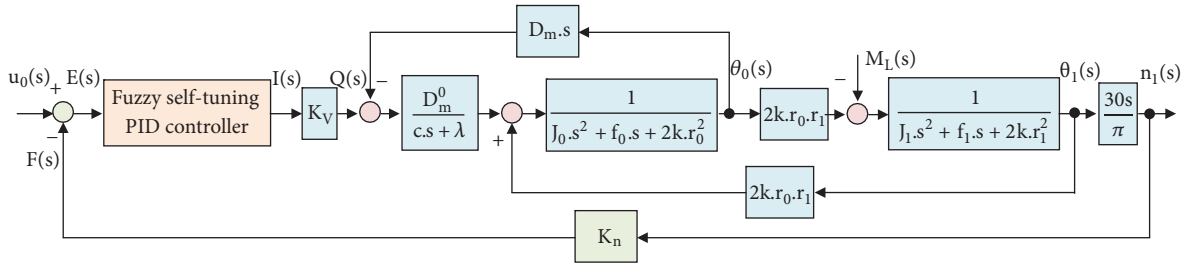

Figure 5: Block diagram.

$$\begin{aligned} Q &= K_V.I; \\ F &= K_n.n_1; \\ n_1 &= \frac{30}{\pi}.\Omega_1; \\ \Omega_1 &= \frac{d\theta_1}{dt}; \\ E &= u_0 - F \end{aligned} \tag{7}$$

From (7), we have

$$\begin{aligned} &2k.r_1.\left[r_0.\theta_0(s) - r_1.\theta_1(s)\right] \\ &\quad = \left(J_1.s^2 + f_1.s\right).\theta_1(s) + M_L(s) \Longleftrightarrow \\ &2k.r_1.r_0.\theta_0(s) = \left(J_1.s^2 + f_1.s + 2k.r_1^2\right).\theta_1(s) + M_L(s) \\ &D_m^0.p(s) \\ &\quad = \left(J_0.s^2 + f_0.s\right).\theta_0(s) + 2k.r_0.\left[r_0.\theta_0(s) - r_1.\theta_1(s)\right] \Longleftrightarrow \\ &D_m^0.p(s) \\ &\quad = \left(J_0.s^2 + f_0.s + 2k.r_0^2\right).\theta_0(s) - 2k.r_0.r_1.\theta_1(s) \\ &Q(s) = D_m.s.\theta_0(s) + (c.s+\lambda).p(s) \\ &Q(s) = K_V.I(s); \\ &F = K_n.n_1(s); \\ &n_1(s) = \frac{30}{\pi}.\Omega_1(s); \\ &\Omega_1(s) = s.\theta_1(s); \\ &E(s) = u_0(s) - F(s) \end{aligned} \tag{8}$$

From (8), we can build the block diagram of the system as shown in Figure 5.

In the theoretical model, we just indicate the relationship between the output signal n_1 with input signal u_0.

2.3. Application of Self-Tuning Fuzzy PID Controller. In this paper, the authors used the fuzzy self-tuning PID controller, such as K_P, K_I, K_D parameters of the classical PID controller, are adjusted by using the fuzzy detector [9]. The cconfiguration of the fuzzy self-tuning PID controller is presented

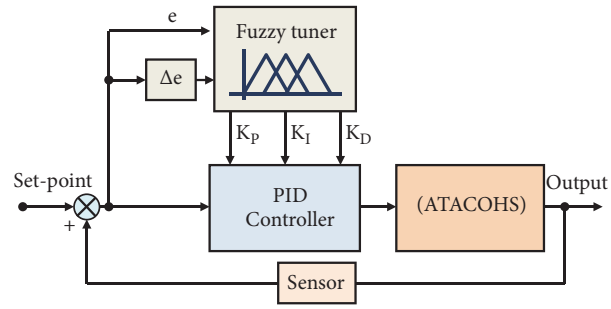

Figure 6: Block diagram of a fuzzy self-tuning PID controller.

in Figure 6. Where e is the error between input and output, $\Delta e = de/dt$ is the derivative of e as a function of time.

For the configuration of the fuzzy self-tuning PID controller, there are two inputs, e and Δe, and three corresponding outputs, K_P', K_I', and K_D'. Mamdani's fuzzy law and processor are used to obtain the optimal values for K_P, K_I, and K_D. The range of parameters of the PID controller is (K_{Pmin}, K_{Pmax}), (K_{Imin}, K_{Imax}), (K_{Dmin}, K_{Dmax}) and is obtained experimentally on the classical PID controller of ATACOHS. The process of finding the PID controller parameter is conducted at the temperature varying from 40°C to 80°C. Initially, we assume $K_I = 0$, $K_D = 0$ and then gradually increase the K_P value until satisfying the set limit of the interval of the speed (within an error of 5% of the set values). Then, we choose the average of K_P and adjust K_D. With the same method, we conduct the experiment with K_P and K_D so that it is within the acceptable range. Then we choose the average of K_P, K_D and continue to adjust K_I. According to the experiments, the ranges of parameters are obtained as $K_P \in (0.033, 0.153)$, $K_I \in (0, 0.0001)$, $K_D \in (0, 0.04)$. So, these parameters can be adjusted in the range (0,1) as [30]

$$\begin{aligned} K_P' &= \frac{K_P - K_{P\min}}{K_{P\max} - K_{P\min}} = \frac{K_P - 0.033}{0.153 - 0.033}, \\ &\qquad K_P = 0.12K_P' + 0.033 \\ K_I' &= \frac{K_I - K_{I\min}}{K_{I\max} - K_{I\min}} = \frac{K_I - 0}{0.0001 - 0}, \quad K_I = 0.0001K_I' \\ K_D' &= \frac{K_D - K_{D\min}}{K_{D\max} - K_{D\min}} = \frac{K_D - 0}{0.04 - 0}, \quad K_D = 0.04K_D' \end{aligned} \tag{9}$$

Table 2: Fuzzy rules of K_P gain.

e \ Δe	NB	N	Z	P	PB
NB	S	S	S	MS	M
N	S	MS	MS	MS	M
Z	S	MS	M	MB	B
P	M	MB	MB	MB	B
PB	M	MB	B	B	B

Table 3: Fuzzy rules of K_I gain.

e \ Δe	NB	N	Z	P	PB
NB	B	B	B	MS	S
N	B	MB	MB	M	S
Z	MB	MB	M	MS	S
P	M	MB	MS	MS	S
PB	M	MS	S	S	S

The input variables e and Δe are symbolized as NB (Negative Big), N (Negative), Z (Zero), P (Positive), and PB (Positive Big). Based on our repeated tests on the PID set, these values are retained. Each test will have different ranges of e and Δe values, and we choose the range of values that mostly appear. According to characteristics of ATACOHS, the input range of e and Δe is from -50 to 50 and from -600 to 600, respectively. The output variables, K_P, K_I, and K_D, are separated as S (Small), MS (Medium Small), M (Medium), MB (Medium Big), and B (Big) with the range from 0 to 1.

Next, the fuzzy rules [9] of the K_P, K_I, and K_D variables are established as shown in Tables 2, 3, and 4, respectively. We will choose the coefficients that match our ATACOHS. The fuzzy self-tuning PID controller is illustrated in Figures 7 and 8.

By using Matlab/Simulink, the fuzzy self-tuning PID controller is plotted in Figure 9.

3. Experimental Procedure

3.1. Control System. In order to control the system, the Arduino Mega 2560 is used. The Arduino Mega 2560 is an ATmega2560 based microcontroller that allows users to write and upload control programs to it using IDE programming software [23, 31]. The power supply we use in this system is Elenco Electronics XP-620. For the controller to drive Festo Didactic proporional valve, a DAC4921 circuit is used to converts from digital format with 12bit resolution. The DAC4921 amplifies voltage from -5vDC to + 5vDC from Arduino to voltage from -10vDC to +10vDC. The control block diagram of the system is shown in Figure 10. Based on the selection equipment, the assembly circuit diagram of the control system is shown in Figure 11.

3.2. Experiments. As discussed in previous parts, for simulation, the system parameters and the block diagram are shown in Table 1 and Figure 4, respectively. In the study, the Matlab/Simulink is used for the simulation [24, 25]. Figure 12 shows the Matlab's interface of the simulation and then the data is saved as .mat format.

For experiments, the PID controller automatically adjusts the control parameters by the algorithm with the program. The control program is written to the Arduino board by IDE programming software. The Arduino board connects to the computer via the virtual COM port and a physical USB connection. The Matlab/Guide interface is built-in functions and procedures for data communication via COM ports [24, 25] as shown in Figure 13. At least five experiments were examined under each condition and the results were averaged to reduce the experimental error and to get reliable results. Finally, the control and feedback signals are stored in.mat format.

4. Simulation and Experimental Tests

4.1. Results and Disscussions. Figure 14 represents the result of a theoretical and empirical investigation of the speed control of the working shaft driven by a hydraulic motor whose speed is controlled by a proportional valve. The results show the difference of velocity response for setting point, simulation, and experiment at five setting speeds, 300, 500, 700, 900, and 1100 rpm. Indeed, the experimental results for the spindle speed control work absolutely in line with the theoretical survey results. We observe that the difference between the corresponding values are in the range of 0.001 to 0.036%; the difference is very small indicating that the experimental results are well consistent with the theoretical conclusion. Furthermore, the comparison between the simulation and experimental results at five setting speeds is shown in Table 5. From the table, the K_P, K_I, and K_D self-tuning parameters of the controller work very well which means that the speed control range from 300 to 1100 rpm of the working shaft

Table 4: Fuzzy rules of K_D gain.

e \ Δe	NB	N	Z	P	PB
NB	S	S	S	MB	B
N	S	MS	MS	M	B
Z	MS	MS	M	MB	B
P	M	MS	MB	MB	B
PB	M	MB	B	B	B

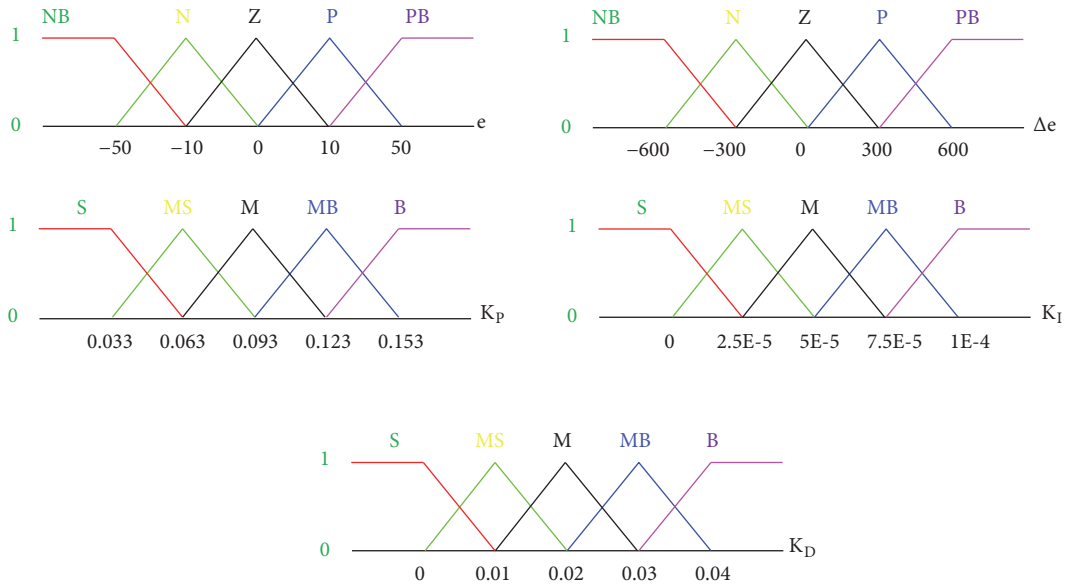

Figure 7: Fuzzy sets of a fuzzy self-tuning PID controller.

ensures no overshoot and the steady state error is less than 5%.

Compared to our result in the previous research [32], when using fixed PID parameters the system worked well for the set point of 2200 rpm (K_P = 0.06, K_I = 0.01, K_D = 0.04). However, with the set points of 600 rpm and 1000 rpm, the system has overshot. This indicated that the classic PID parameters only work well for certain value.

To confirm that the self-tuning fuzzy PID parameter on our system is working well when one of the uncertainty factors, such as the increase of the temperature of the oil, the change of oil viscosity during the operation period, the oil losses in the pipeline, oil leaks inside the hydraulic elements. In this paper, we only consider the effect of temperature on the response of the system.

In addition, in this study, in order to demonstrate that the self-tuning fuzzy PID controller works well for the large temperature range in comparison with [1], the effect of the oil temperature is investigated. The temperature varies from 40 to 80°C on the work shaft when it rotates at 500, 900 rpm on the experimental model. In this paper, we only change the oil temperature to investigate speed stability of the working shaft and other parameters of working oil such as viscosity, chemical and physical stability, lubrication ability, and foaming are neglected.

The transient responses of the speed of the working shaft at 5 difference temperatures (40°C, 50°C, 60°C, 70°C, and 80°C) and 2 speed values (500rpm and 900 rpm) are shown in Figures 15–19. Also, in order to investigate the effect of oil temperature on velocity response, some comparison values such as set speed, actual speed, overshoot, delay, settling time, and error are provided in Table 6. The results show that, at low temperature from 40°C to 50°C, the delay time is greater than when controlled at temperatures above 50°C, 0.02 compared with 0.01sec at temperature lower and higher than 50°C, respectively. Also, at temperature from 50°C to 70°C, it shows a very good response, in particular, the delay time is 0.01 sec, and fast response time increases from 2.53 to 2.57 seconds at 500 rpm and decreases from 2.72 to 2.61 seconds at 900 rpm. The error in number of revolutions for the upper and lower limits is lower than that in the other temperature range (≤ 50°C and ≥ 80°C). When the temperature is greater than 80°C, the rotation error at the steady state increases. This is suitable because the viscosity of oil is reduced at high temperatures; thus, it results in higher loss. Figures 14–19 show that the working shaft speed has little oscillates at steady state. However, the range of fluctuation is still less than 5% which is the criterion of the transient response of the system. It is clear that the velocity response of the working shaft is still good when the fuzzy self-tuning PID controller is used.

Table 5: Theoretical and experimental results.

Setting speed (rpm)	Methodology	Results					
		Acutal speed (rpm)	*Overshoot (%)*	*Delay time (s)*	*Setting time (s)*	*Upper bound error (%)*	*Lower bound error (%)*
300	Theory	300.1	0	0	2.53	1.5	0
	Experiment	300±10	0	0.02	2.63	3.3	3.6
500	Theory	500.2	0	0	2.54	1.5	0
	Experiment	500±10	0	0.02	1.87	3	2
700	Theory	700.2	0	0	2.53	1.5	0
	Experiment	700±10	0	0.01	3.16	2	3.5
900	Theory	900.4	0	0	2.54	1.5	0
	Experiment	900±10	0	0.01	2.96	2.2	2.2
1100	Theory	1101	0	0	2.43	1.5	0
	Experiment	1100±10	0	0.01	3.32	1.9	2.6

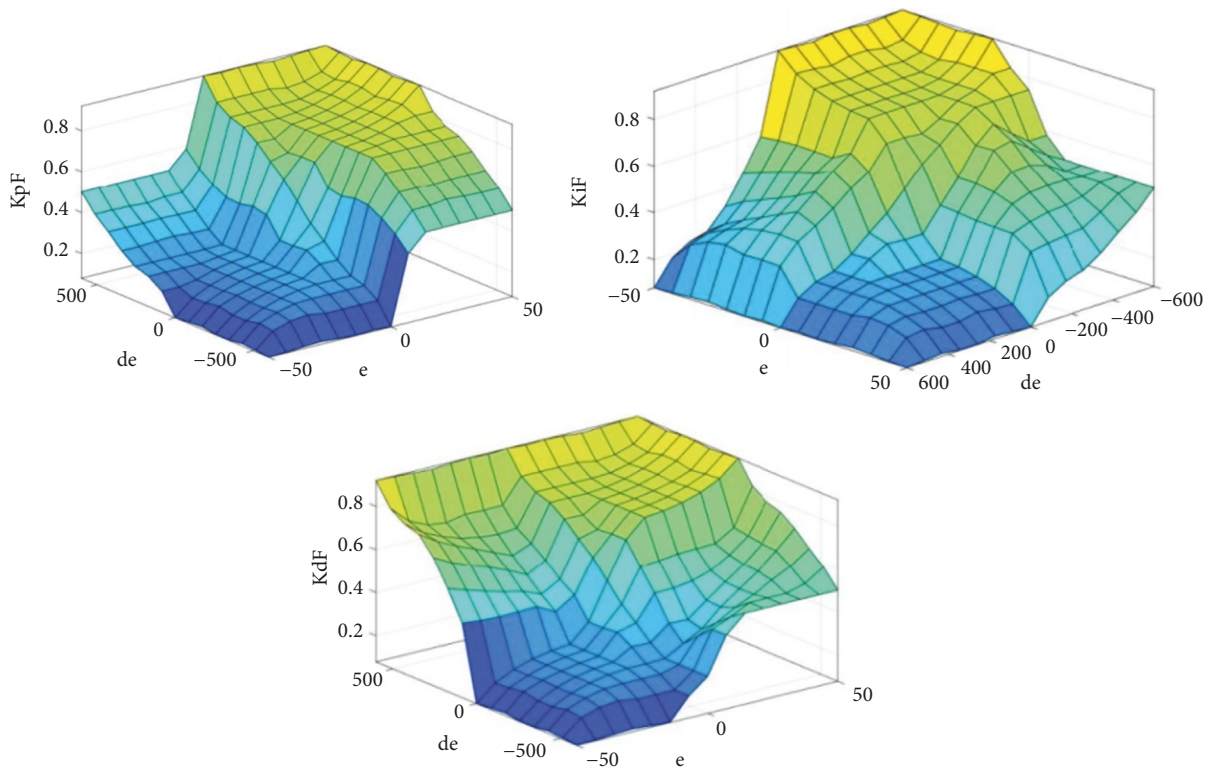

Figure 8: The ouput variables of the fuzzy self-tuning PID controller.

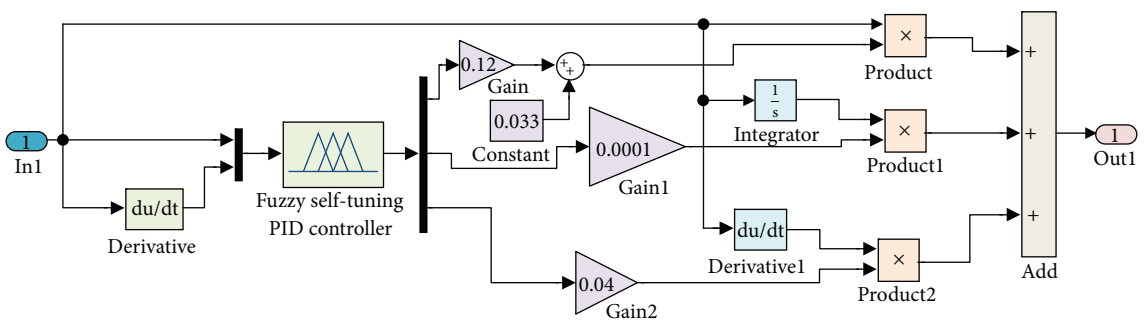

Figure 9: Fuzzy self-tuning PID simulation in Matlab/Simulink.

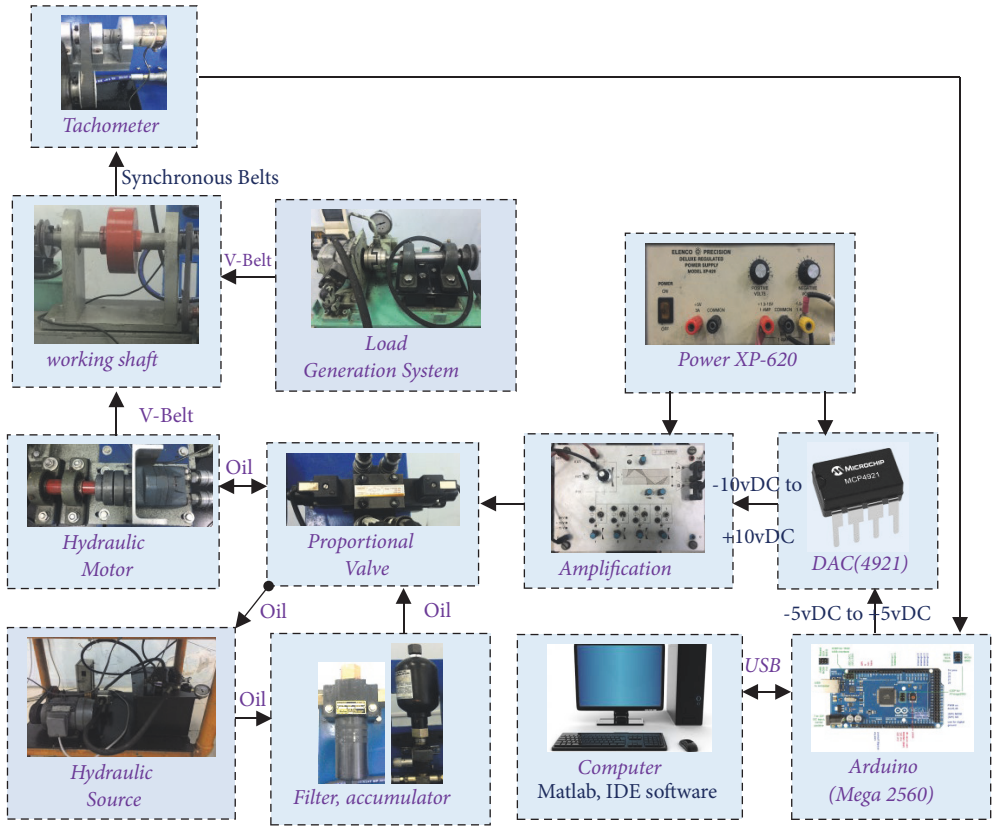

Figure 10: Control block diagram.

Table 6: Experimental results as a function of the oil temperature.

Oil temperature (°C)	Setting speed (rpm)	Results					
		Actual speed (rpm)	*Overshoot (%)*	*Delay time (s)*	*Setting time (s)*	*Upper bound error (%)*	*Lower bound error (%)*
40(±2)	500	500±10	0	0.02	3.5	2.6	2.8
	900	900±10	0	0.02	3.2	2.2	1.6
50(±2)	500	500±10	0	0.02	3.04	2.6	2.4
	900	900±10	0	0.02	3.25	1.8	1.4
60(±2)	500	500±10	0	0.01	2.57	2.7	2.3
	900	900±10	0	0.01	2.75	1.7	2.4
70(±2)	500	500±10	0	0.01	2.53	2.5	2.4
	900	900±10	0	0.01	2.61	1.8	2.4
80(±2)	500	500±10	0	0.01	2.69	3.6	2.6
	900	900±10	0	0.01	2.07	1.9	2.5

On the other hand, in practice, the Kp, Ki, Kd coefficients are good but vary exponentially (asymptotic to the input signal). Therefore, at high temperatures, the viscosity of the oil and the oil friction on the tube wall decreases; the opening of the valve also decreases, leading to the oil flow through the valve to the hydraulic motor increases, so the response time of the system is faster (shown in the dynamic properties of Figures 15–19 and Table 6). This issue fits in with the findings of Fouly A. and Guy [17].

According to the results of Ali Abdul Mohsin Hassan et al. [1], the response at 700 rpm with the temperature range of 60-70°C is the best result. From their results and our previous results [32], it has been confirmed that classical PID control with fixed parameter is only suitable to work on a certain speed and corresponds to a variable range of parameters during the operation. This is a limitation when applied on the spindle of a metal cutting machine because when machining a workpiece with multiple surfaces, each

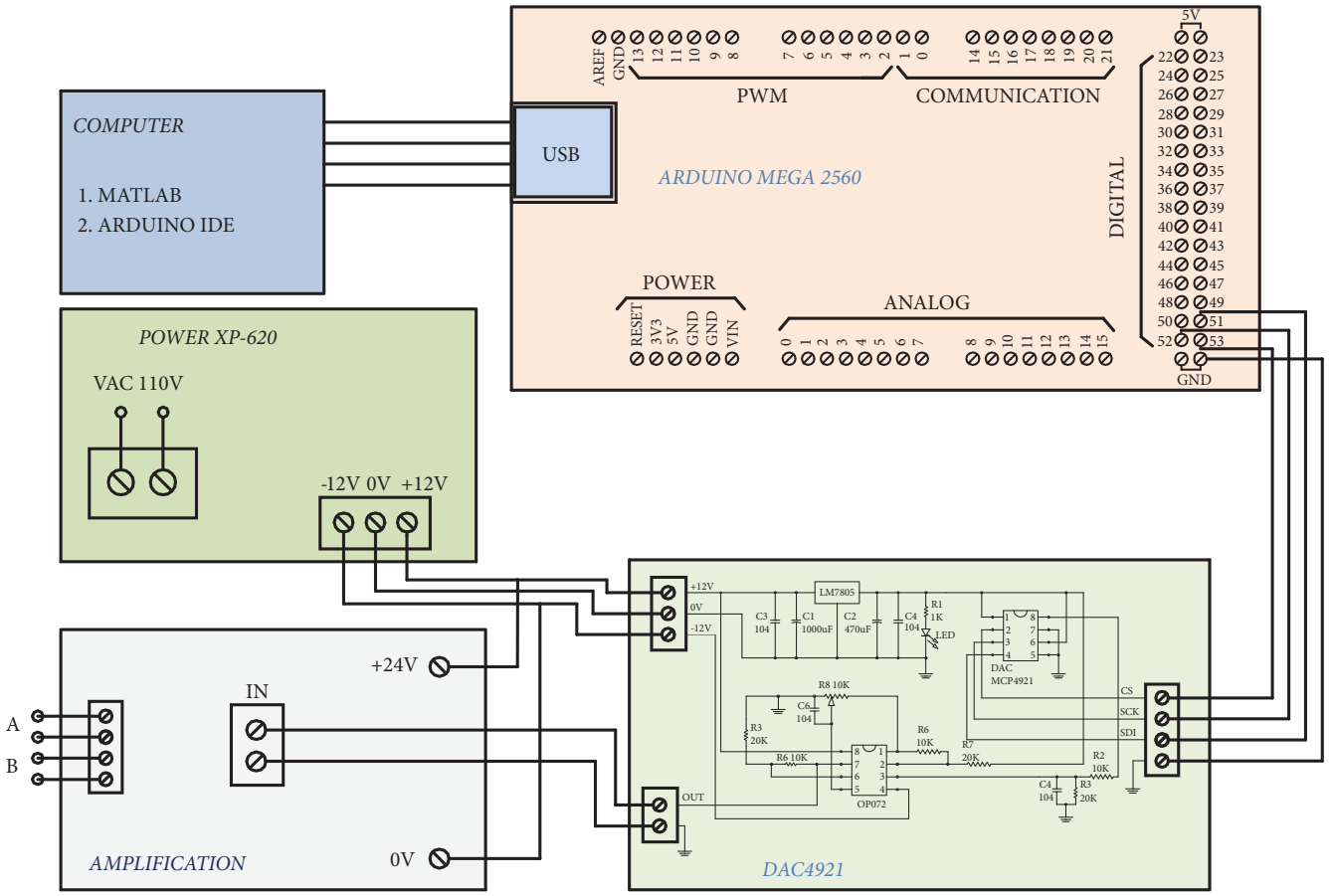

Figure 11: Assembly circuit.

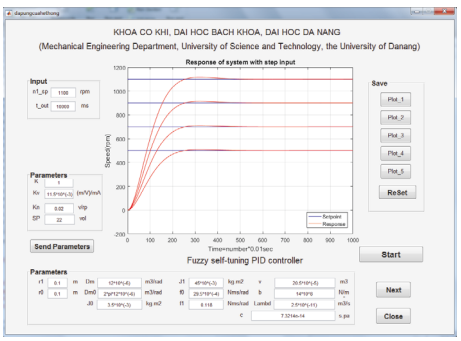

Figure 12: Simulating result on Matlab/Guide.

of which has a different machining size, the cutting speed must be appropriate to ensure the quality of the final product. Thus, in the machining process, it is necessary to change the rotation speed of the spindle corresponding to each size of work. Therefore, the PID self-adjusting controller application fully complies with our proposed system.

4.2. Application to Metal Cutting Machine. The test machine we propose is a lathe machine which uses hydraulic drive for the spindle. The system is compared to the one that has the spindle driven by a 3-phase electric motor via an inverter. A photo of the test machine is shown in Figure 20.

Table 7: Machining parameters selection.

Spindle drive	Machining parameter
Three-phase electric motors drive	n_{tc} = 1100(rpm) S = 30(mm/min)
Hydraulic motor drive	t = 0.2(mm)

The size and details of the workpiece are shown in Figure 21; the selected material is CT38 steel.

Choose cutting tool and machining parameters according to Mitsubishi standard, as shown in Table 7.

The machining of 3 different samples on each system, i.e., a total of 6 samples, was taken, where the samples 1-3 are machined with hydraulic drive system and the samples 4-6 machined with three-phase electric motor system. The measurement of 6 specimens was processed on the measuring machine Mitutoyo Surftest SJ-301. The details of speciments and of the measurement are shown in Figure 22.

The results of the samples 1, 2, and 3 are shown in Table 8 and the values for Rz and its graphs are on Figure 23.

The results of the samples 4, 5, and 6 are shown in Table 9 and the values for Rz and its graphs are on Figure 24.

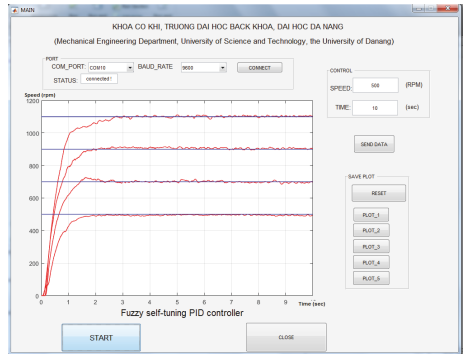

Figure 13: Experimental result on Matlab/Guide.

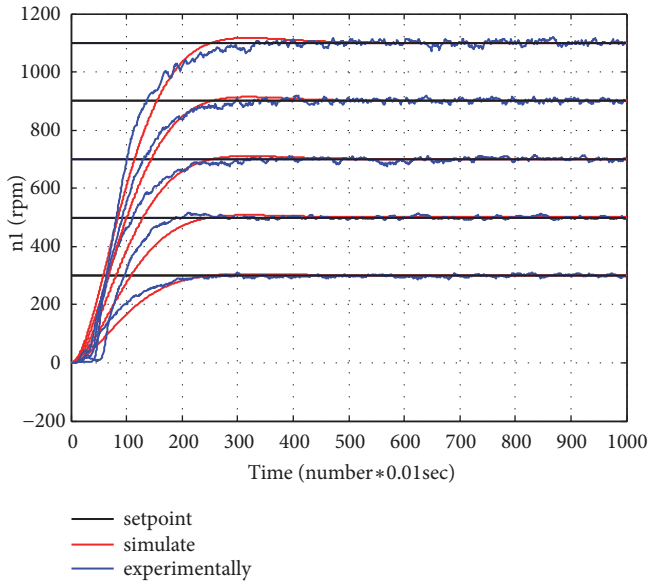

Figure 14: Velocity respone of the working shaft.

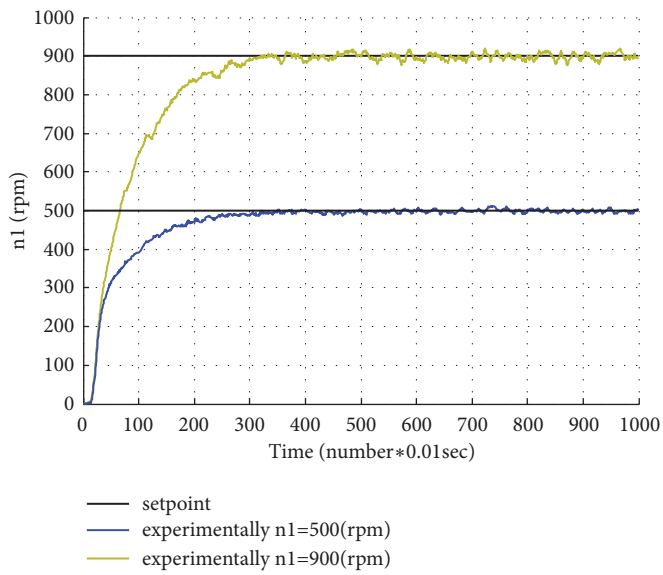

Figure 15: Velocity respone of the working shaft at oil temperature of 40°C.

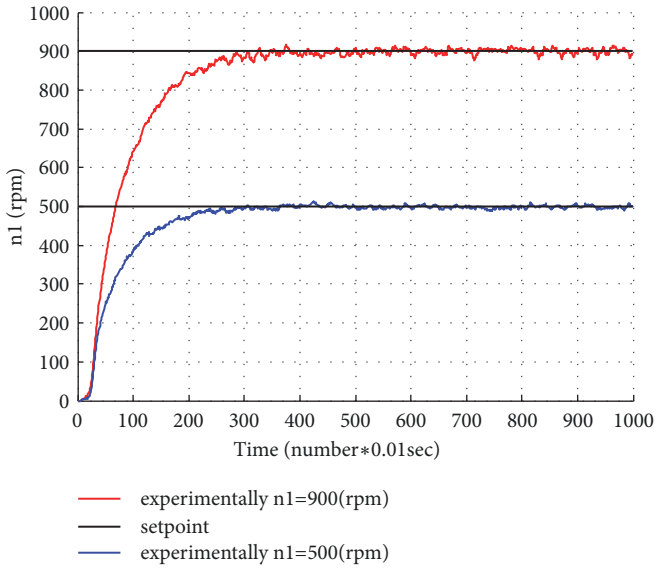

Figure 16: Velocity respone of the working shaft at oil temperature of 50°C.

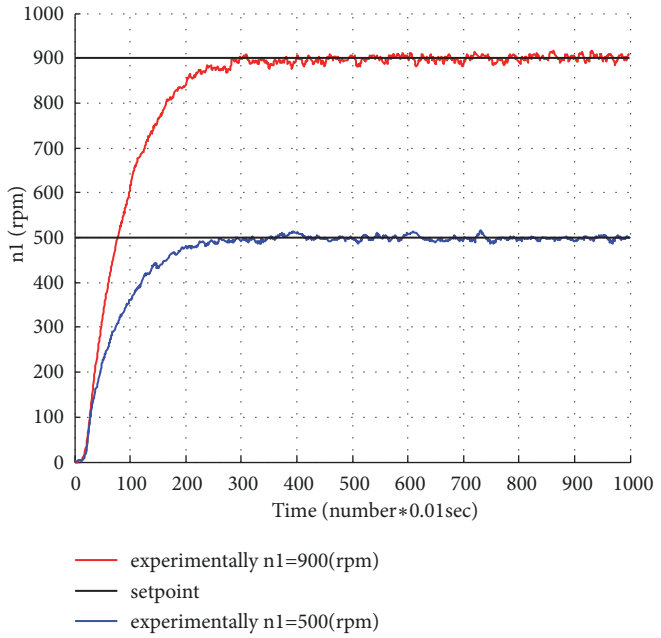

Figure 17: Velocity response of the working shaft at oil temperature of 60°C.

Table 8: Surface roughness results for samples 1, 2, and 3.

Machining parameters	Sample	Surface roughness Rz (μm)	Average of Rz (μm)	Roughness Grade
n_{tc}= 1100(rpm)	1	21.427		
S= 30(mm/min)	2	21.331	21.381	~ 5
t= 0.2(mm)	3	21.385		

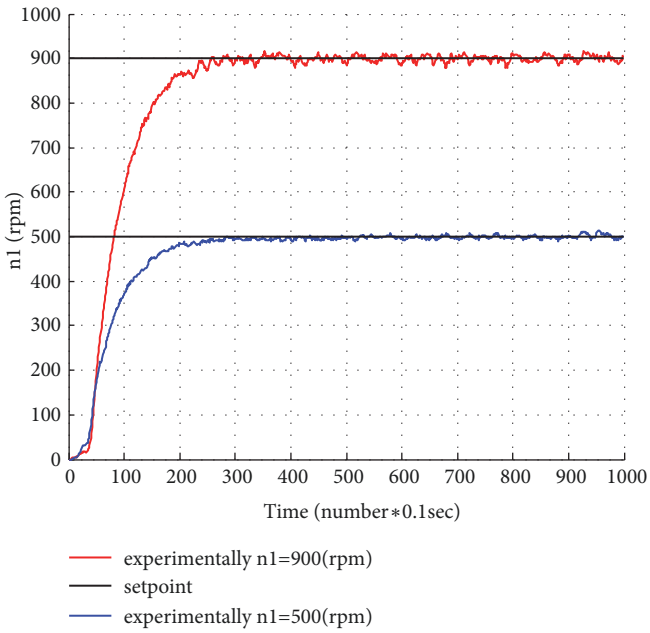

Figure 18: Velocity response of the working shaft at oil temperature of 70°C.

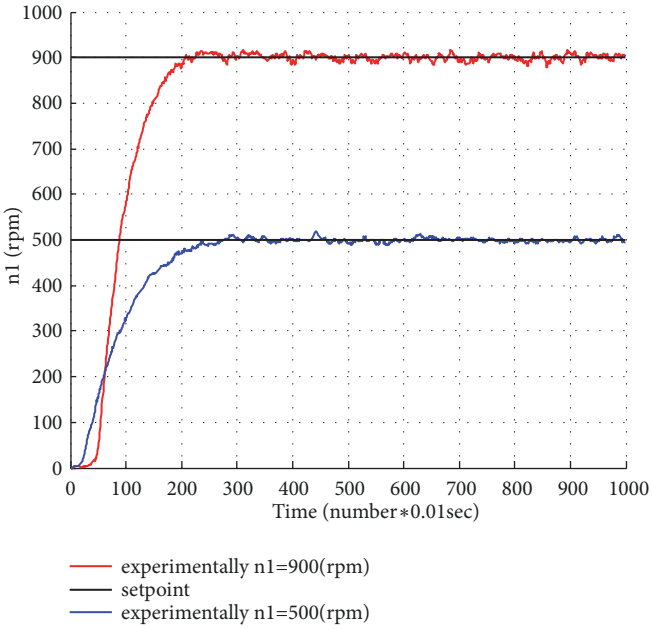

Figure 19: Velocity response of the working shaft at oil temperature of 80°C.

On Table 8, we found that the 3 samples had the same roughness and the average was 21.381 (μm). On the other hand, the profile in the graph (Figure 23) was relatively uniform, according to the corresponding standard (grade 5).

Similarly, on Table 9, with the same machining parameters, we find that the 3 machined samples have the average roughness value of 26.535 (μm). The profile for each sample is almost the same and the roughness grade is 5 as shown in Figure 24.

Based on the above results, we found that, with the same machining process on the two spindle drive systems, the surface roughness was in the same grade (grade 5).

5. Conclusions

In this paper, a new model for the working shaft transmission was designed and built. Then, the mathematical equations

Table 9: Surface roughness results for samples 4, 5, and 6.

Machining parameters	Sample	Surface roughness Rz (μm)	Average of Rz (μm)	Roughness Grade
n_{tc}= 1100(rpm)	4	27.105		
S= 30(mm/min)	5	27.568	26.5353	~ 5
t= 0.2(mm)	6	24.933		

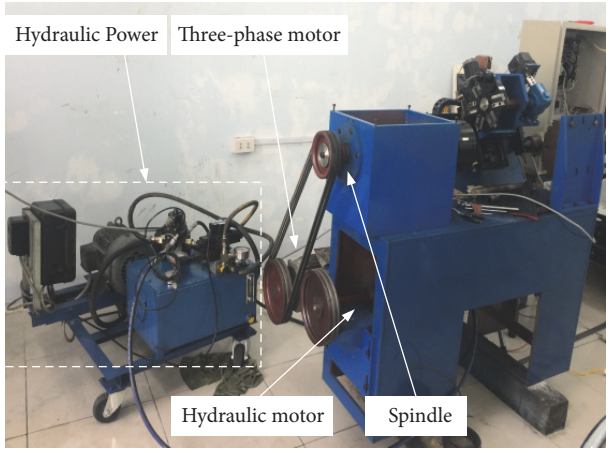

Figure 20: Picture of experimental equipment.

for the signals of the system can be obtained. Furthermore, the fuzzy self-tuning PID controller with the K_P, K_I, and K_D parameters is chosen for the velocity response of the working shaft (at different setting speed). This study took into account the set of influenced parameters such as the moment of mass inertia of the work shaft assembly; the friction on the work axis; the moment of mass inertia of rotor and viscous friction on the rotational axis of hydraulic engine; and the elastic deformation of the transmission belt from the hydraulic motor to the work axis. The test-rig of ATACOHS is built and the control program is developed. Based on the experimental results, the following conclusions can be made:

(1) We proposed a model of two rotational masses and two elastic stages with mathematical descriptions showing the relationship between the input and output signals in the system.

(2) Fuzzy PID parameters have been found to control the system at different setting speeds.

(3) The effect of oil temperature (from 40°C to 80°C) to the velocity response of the working shaft is considered (this is to confirm that the PID self-adjusting controller is appropriate for our particular application). The transient response of ATACOHS shows a good trend. However, it is better if the temperature of the oil is not higher than 70°C.

(4) The highlight of this paper is that we have applied ATACOHS on the spindle of the lathe with the mostly same results of surface roughness with reference to the three-phase electric system. This result will apply the new transmission system for the spindle of the metal cutting tool, and the hydraulic motor system for the spindle will be synchronous with the tool-feeder hydraulic cylinder drive that the manufacturers are currently used.

(5) The ATACOHS can be developed to apply for controlling the spindle of metal cutting machines and specialized high capacity CNC machines because it has many oustanding features such as compact structure, simple to operate, and stepless controls of the spindle speed without the need of a gearbox.

(6) In the next publication, we will introduce the relationship between the output signal n_1 and the input

Table 10: Abbreviation.

Symbol	Description
ATACOHS	Automatic transmission and control of hydraulic systems
$W_{ĐK}$	Controller
PID	Proportional-Integral-Derivative controller
DAC	Digital-to-analog converter
IDE	Integreted Development Environment
K_p	is the proportional gain, a tuning parameter
K_I	is the integral gain, a tuning parameter
K_D	is the derivative gain, a tuning parameter
e	Error
NB	Negative big
N	Negative
Z	Zero
P	Positive
PB	Positive big
S	Small
MS	Medium Small
M	Medium
MB	Medium Big
B	Big

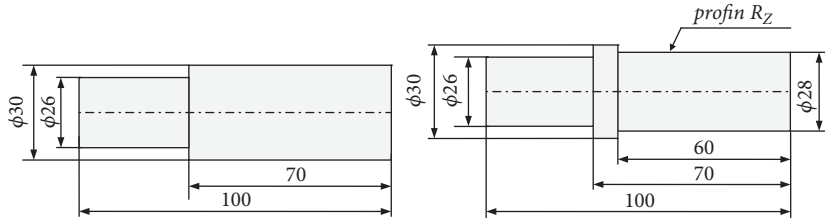

Figure 21: Workpiece configuration for machining (CT38).

Figure 22: Details and R_Z profiling process of 06 detailed samples.

Figure 23: Pictures of Rz and profin graph of samples 1,2,3.

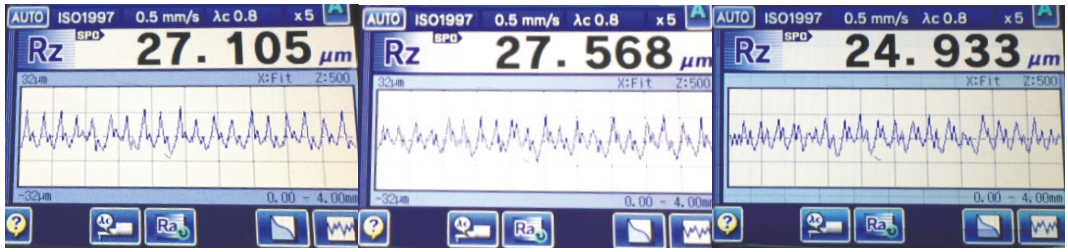

Figure 24: Pictures of Rz and profin graphs of samples 4, 5, 6.

signal M_L. The proposed experimental model is the hydraulic spindle lathe driven by hydraulic motors. The next study will include the investigation of ATACOHS dynamics through the quality of surface roughness of machined parts in which the reference spindle drive system is a three-phase electric motor.

Appendix

See Table 10.

Data Availability

The data used to support the findings of this study are available from the corresponding author upon request.

Conflicts of Interest

The authors declare that they have no conflicts of interest.

Acknowledgments

The authors would like to extend their sincere thanks to staffs at the Institute of Mechanical and Automation, Danang

University of Science and Technology, Vietnam, for the supports and experimental tests.

References

[1] A. A. M. H. AL-Assady and T. J. A. Mohammad, "Design and analysis of electro-hydraulic servo system for speed control of hydraulic motor," *Journal of Engineering*, vol. 5, pp. 562–573, 2013.

[2] M. E. Graham Jr. and L. Ronnie, "Electro-Hydraulic position control for a machine tool with actual and commanded position feedback," *International Journal of Machine Tool Design and Research*, vol. 26, 1986.

[3] A. M. Minar, A. Gullu, and S. Taskin, "Statistical investigation of hydraulic driven circular interpolation motions," *Indian Academy of Sciences*, vol. 37, pp. 557–568, 2012.

[4] C. C. Mbaocha, Lakpah E. A., and A. E. Jonathan, "A numerical machine tool controller for servomechanisms," *International Journal of Scientific and Research Publications*, vol. 5, pp. 1–4, 2015.

[5] http://www.senday.com.tw/en/feeding01.html.

[6] http://mt.fuji.co.jp/e/products/hardturning/.

[7] A. C. Kong, X. Zhang, and G. L. Hao, "Simulation study on constant speed output control of fixed displacement pump-variable displacement motor hydraulic system," in *Proceedings of the International Conference on Fluid Power and Mechatronics, FPM 2011*, pp. 276–281, China, August 2011.

[8] H. W. Wu and C. B. Lee, "Influence of a relief valve on the performance of a pump/inverter controlled hydraulic motor system," *Mechatronics*, vol. 6, no. 1, pp. 1–19, 1996.

[9] I. Sohail, N. Boumella, and C. F. G. Jua, *A Hybrid of Fuzzy and Fuzzy Self-Tuning PID Controller for Servo Electro-Hydraulic System*, InTech, 2012.

[10] M. Xu, B. Jin, G. Chen, and J. Ni, "Speed-control of energy regulation based variable-speed electrohydraulic drive," *Strojniski Vestnik: Journal of Mechanical Engineering*, vol. 59, no. 7-8, pp. 433–442, 2013.

[11] R.-F. Fung, Y.-C. Wang, R.-T. Yang, and H.-H. Huang, "A variable structure control with proportional and integral compensations for electrohydraulic position servo control system," *Mechatronics*, vol. 7, no. 1, pp. 67–81, 1997.

[12] A. A. Ayman, "Self tuning fuzzy logic control of an electrohydraulic servo motor," *ACSE Journal*, vol. 5, no. 4, pp. 67–76, 2005.

[13] P. Pornjit, T. Siripun, and T. Surapun, "A hybrid of fuzzy and proportional-integral-derivative controller for electro-hydraulic position servo system," *Energy Research Journal*, vol. 1, no. 2, pp. 62–67, 2010.

[14] K. Majid, N. Farid, S. Hossein, and S. Mozafar, "Application of a flexible structure artificial neural network on a servo-hydraulic rotary actuator," *International Journal of Advanced Manufacturing Technology*, vol. 39, pp. 559–569, 2008.

[15] H. M. Khalil and M. El-Bardini, "Implementation of speed controller for rotary hydraulic motor based on LS-SVM," *Expert Systems with Applications*, vol. 38, no. 11, pp. 14249–14256, 2011.

[16] M. F. Rahmat, S. M. Rozali, N. A. Wahab, Zulfatman, and K. Jusoff, "Modeling and controller design of an electro-hydraulic actuator system," *American Journal of Applied Sciences*, vol. 7, no. 8, pp. 1100–1108, 2010.

[17] A. Fouly, T. W. Sadak et al., *Effect of Oil Temperature on the Performance of A Hydraulic Linear System Controlled with Electro Hydraulic Servo Valve*, Department of Production and Design Engineering, Minia University, 2015.

[18] H. E. Merritt, *Hydraulic Control Systems*, Wiley, New York, NY, USA, 1967.

[19] E. J. Mohieddine and K. Andreas, *Hydraulic Servo-Systems*, Springer, London, UK, 2004.

[20] L. Rong, L. Jing, S. Chun-geng, and L. Sen, "Analysis of electro-hydraulic proportional speed control system on conveyer," *Procedia Engineering*, vol. 31, pp. 1185–1193, 2012.

[21] K. Dasgupta and H. Murrenhoff, "Modelling and dynamics of a servo-valve controlled hydraulic motor by bondgraph," *Mechanism and Machine Theory*, vol. 46, no. 7, pp. 1016–1035, 2011.

[22] B. B. Ghosh, B. K. Sarkar, and R. Saha, "Realtime performance analysis of different combinations of fuzzy-PID and bias controllers for a two degree of freedom electrohydraulic parallel manipulator," *Robotics and Computer-Integrated Manufacturing*, vol. 34, pp. 62–69, 2015.

[23] https://www.arduino.cc/en/Guide/Windows.

[24] https://uk.mathworks.com/products/MATLAB.html.

[25] http://playground.arduino.cc/Interfacing/MATLAB.

[26] B. Eryilmaz and B. H. Wilson, "Unified modeling and analysis of a proportional valve," *Journal of The Franklin Institute*, vol. 343, no. 1, pp. 48–68, 2006.

[27] C. Peter, *Principles of Hydraulic Systems Design*, Momentum Press, LLC, New York, NY, USA, 2015.

[28] K. C. Gustavo and S. Nariman, *Hydrostatic Transmissions and Actuators*, Wiley, 2015.

[29] C. D. Richard and H. B. Robert, *Modern Control Systems*, Pearson Prentice Hall, Upper Saddle River, 12th edition, 2010.

[30] N. Tran, C. Le, and A. Ngo, "Experimental investigation of speed control of hydraulic motor using proportional valve," in *Proceedings of the International Conference on System Science and Engineering (ICSSE)*, pp. 330–335, Ho Chi Minh City, Vietnam, July 2017.

[31] http://binaryupdates.com/how-to-setup-and-program-arduino-board/.

[32] N. H. Tran, C. Le, and A. D. Ngo, "Experimental study on speed stability of lathe spindle driven by hydraulic motor," in *Proceedings of the 6th National Conference on Mechatronics*, pp. 494–499, Vietnam, 2016.